

Electronic Supplementary Information

High quantum efficiency Ce:(Lu,Y)₃(Al,Sc)₂Al₃O₁₂ transparent ceramics with excellent thermal stability for high power white LEDs/LDs†

Yuelong Ma^{a,b}, Le Zhang^{a,c,d,*}, Tianyuan Zhou^a, Chen Hou^a, Jian Kang^a, Shunshun Yang^a,
Xiaoqian Xi^a, Mingxing Yuan^a, Jin Huang^a, Rui Wang^a, Farida A Selim^c, Ming Li^d, Yun
Wang^b, Hao Chen^{a,*}

a. Jiangsu Key Laboratory of Advanced Laser Materials and Devices, School of Physics
and Electronic Engineering, Jiangsu Normal University, Xuzhou, 221116, P.R. China

b. School of Mechanical Engineering, Jiangsu University, Zhenjiang, 212013, P.R. China

c. Department of Physics and Astronomy, Bowling Green State University, Bowling Green,
43403, USA

d. Department of Mechanical, Materials and Manufacturing, University of Nottingham,
Nottingham NG14BU, UK

E-mail: zhangle@jsnu.edu.cn (Le Zhang); chenhao@jsnu.edu.cn (Hao Chen)

† Electronic Supplementary Information (ESI) available: See DOI: 10.1039/x0xx0000x

1 Supporting Table

Table S1 Spectral shift, thermal stability and quantum efficiency in the previously reported Ce³⁺ doped garnet.

Year	Researchers	Garnet components	Wavelength shift	QE	thermal stability (at 150 °C)	Ref.
2019	Zou et al.	GdYAG:Ce	33 nm	-	Loss 50%-80%	[15]
2019	Xie et al.	Gd ₃ (Ga,Al) ₅ O ₁₂	-	~50%	Loss ~50%	[26]
2019	Jiang et al.	Ce:YAGG	Blue-shift 50 nm	79.1%	Loss 80%	[19]
2019	Liu et al.	Lu ₂ Mg ₂ Al ₂ Si ₂ O ₁₂ :Ce	-	63.4%	Loss 19%	[21]
2019	Zhou et al.	(Tb,Gd) ₃ Al ₅ O ₁₂ :Ce	21 nm	-	-	[18]
2020	Zhou et al.	Y ₃ (Mg _{1.8} Al _{1.4} Si _{1.8})O ₁₂ :Ce	14 nm	-	Loss 36% at 450 K	[20]
2020	Zhu et al.	YAGG:Ce-YAG	-	68.3%	Loss 10%	[24]

Table S2 Phase compositions and spectral properties in the previously reported Sc³⁺ doped garnet.

Year	Researchers	Garnet components	Wavelength shift	FWHM	Phase composition	Ref.
2011	Boulesteix et al.	Nd:Y ₃ ScAl ₄ O ₁₂	-	increased	Pure garnet	[37]
2012	Petrosyan et al.	>20 at.% Sc:Lu ₃ Al ₅ O ₁₂	-	-	(Lu,Sc) ₂ O ₃ and garnet phase	[40]
2015	Xia et al.	Ce:Lu ₃ Sc ₂ Al ₃ O ₁₂	Blue shift	-	Sc ₂ O ₃ and garnet phase	[39]
2019	Li et al.	Tm:Y ₃ ScAl ₄ O ₁₂	-	increased	Pure garnet	[33]
2019	Li et al.	Yb:Y ₃ ScAl ₄ O ₁₂	-	increased 1.3 times	Pure garnet	[34]
2020	Zhang et al.	Ce:Y ₃ (Al,Sc) ₅ O ₁₂	21 nm	6.5 nm	Pure garnet	[65]

Table S3 Main parameters determined with Rietveld refinements of Ce:LuYSAG TCs.

	ScLu30Y0	ScLu25Y0	ScLu20Y1	ScLu15Y1	ScLu10Y2	ScLu05Y2	ScLu00Y3
	0	5	0	5	0	5	0
Unit cell (Å)	12.09786	12.15912	12.17997	12.20148	12.22348	12.24852	12.26872
Cell volume (Å ³)	1770.623	1797.657	1806.923	1816.507	1826.353	1837.601	1846.705
garnet	91.089%	93.157%	94.188%	100%	100%	100%	100%
Sc ₂ O ₃	8.911%	6.843%	5.812%				
Y/Lu/Ce1- O (Å)	2.4754	2.4607	2.4504	2.4234	2.4434	2.4545	2.4849
Y/Lu/Ce2- O (Å)	2.4328	2.3457	2.3664	2.3584	2.3560	2.3715	2.3802
Al/-O(1) (Å)	2.0323	2.0511	2.0564	2.0554	2.0427	2.0401	2.0778
Al/-O(2) (Å)	1.6514	1.7074	1.7144	1.7284	1.7570	1.7725	1.7869
Reliability factors							
Rwp	7.19%	6.44%	8.80%	7.41%	6.96%	6.75%	7.72%
Rp	5.20%	4.73%	6.71%	5.17%	5.29%	5.32%	5.78%
χ ²	3.38	2.51	4.494	3.16	2.438	1.82	1.737

2 Detailed Fabrication of Transparent Ceramics

In this work, commercial powders of α - Al_2O_3 (4N, Alfa Aesar, Ward Hill, America), Y_2O_3 (4N, Alfa Aesar, Ward Hill, America), Lu_2O_3 (4N, Alfa Aesar, Ward Hill, America), Sc_2O_3 (3N, Shandong Xiya, Shandong, China) and CeO_2 (3N, Shandong Xiya, Shandong, China) were selected as the starting materials to fabricate $\text{Ce}:(\text{Lu},\text{Y})_3(\text{Al},\text{Sc})_2\text{Al}_3\text{O}_{12}$ TCs. 0.5 wt.% tetraethyl orthosilicate (4N, Alfa Aesar, Ward Hill, America) was chosen as the sintering additive.

These powders were mixed with 0.3 wt.% DS005 (99.9 % purity, Alfa Aesar, Ward Hill, America) as a dispersing agent in anhydrous ethyl alcohol in a ball milling jar, and then planetary ball milled for 15 h to obtain powders with a uniform particle size distribution. The mixture was dried at 60 °C in an oven for 24 h, and then meshed and sieved through a 150-mesh screen. After that, the sieved powder mixture was initially uniaxially pressed at 20 MPa in a stainless-steel mold with a diameter of 22 mm, and then cold isostatic pressed at 200 MPa for 300 s, to obtain compacted powder pellets with a relative density of ~53 % of the theoretical value of LuAG. The pressed pellets were then calcined at 800 °C for 4 h in air in a muffle furnace to remove the volatile organic residues. The calcined green bodies were then vacuum sintered (10^{-5} Pa) in a tungsten mesh heated vacuum furnace (712T, Thermal Technology LLC, USA) at 1760 °C for 8 h. After that, the specimens were mirror polished on both surfaces to 1.0 mm-thick.

3 Supporting figures

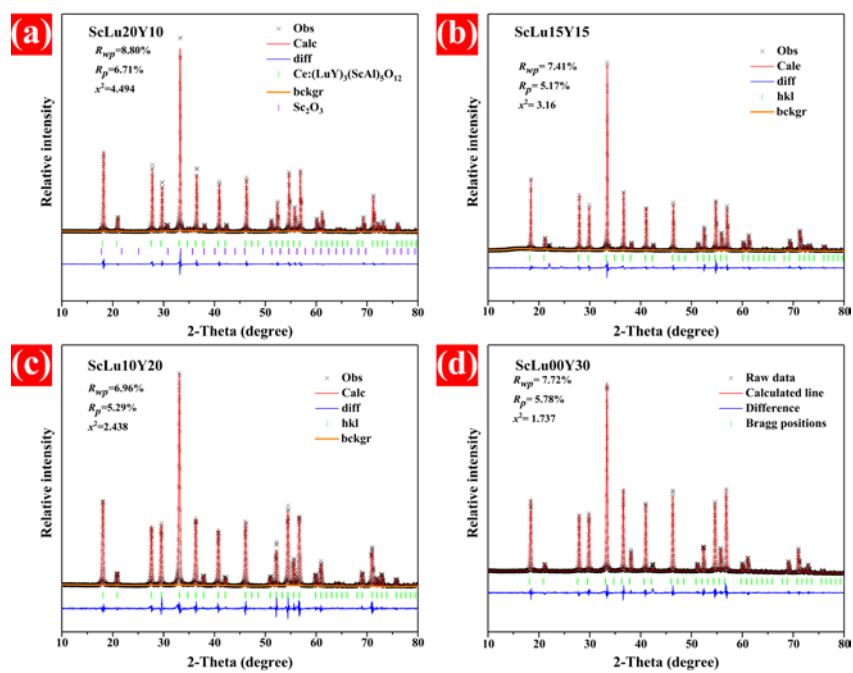


Fig. S1 Rietveld refinement patterns of TCs: (a) ScLu20Y10, (b) ScLu15Y15, (c) ScLu10Y20, (d) ScLu00Y30.

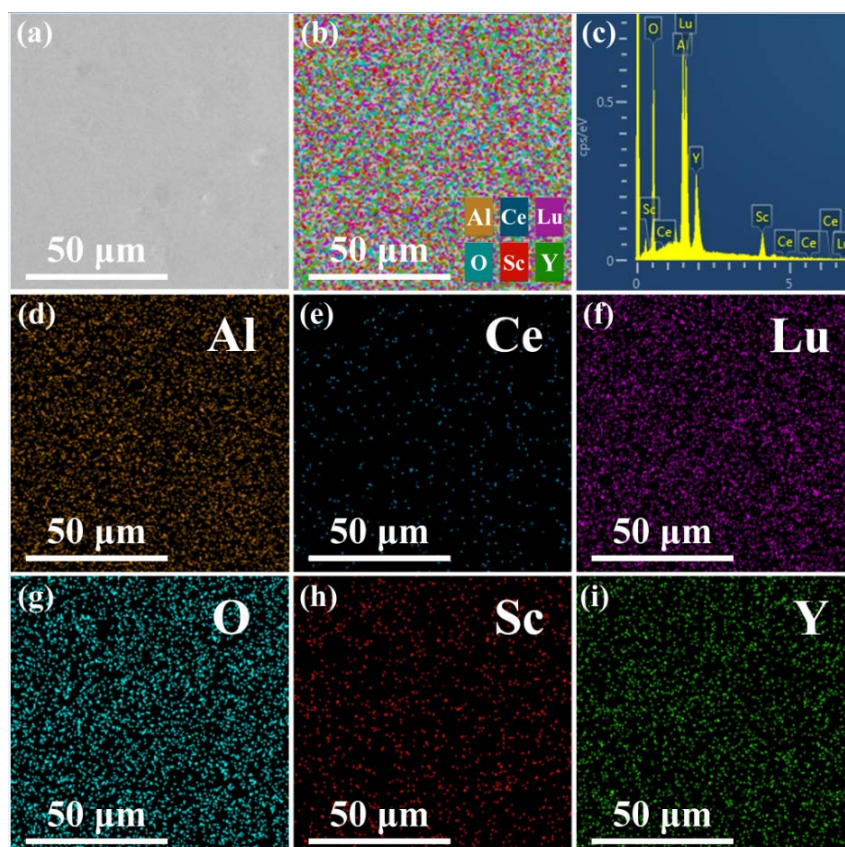


Fig. S2 EDS mapping of the ScLu15Y15 TC.

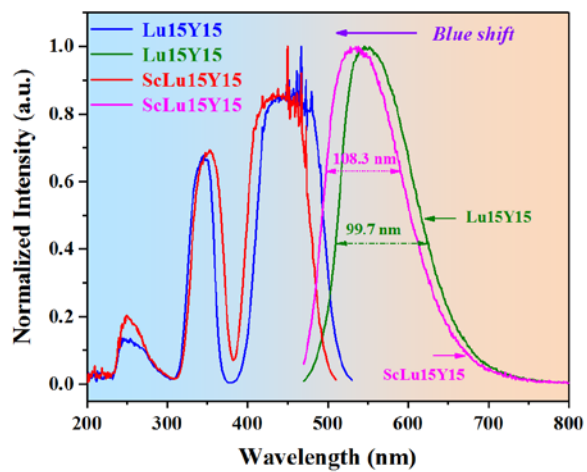


Fig. S3 Normalized PL of Lu15Y15 TC and ScLu15Y15 TCs ($\lambda_{ex}=460$ nm).



Fig. S4 Appearance of Lu15Y15 TC.

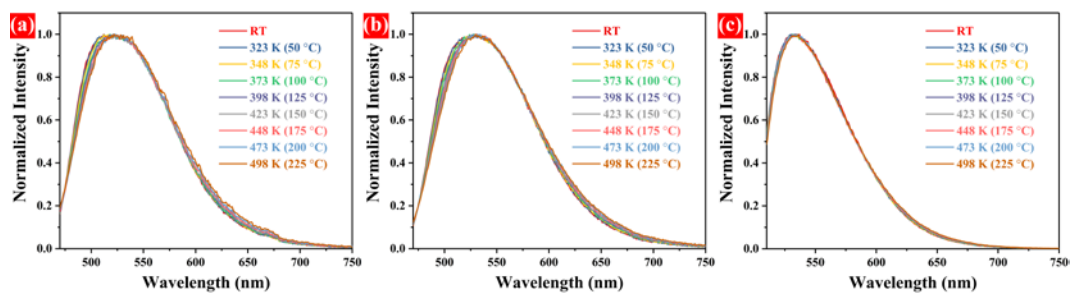


Fig. S5 Normalized temperature-dependent PL intensities of prepared TCs (a)

ScLu30Y00, (b) ScLu20Y10, (c) ScLu15Y15.

To better understand the thermal stability characteristics of TCs, their activation energies (ΔE) were calculated by the Arrhenius equation.

$$I(T) \approx \frac{I_0}{1 + C \exp\left(-\frac{\Delta E}{KT}\right)} \quad (1)$$

Where I_0 and I_T are the emission intensity at RT and the operating temperature, C is a constant, and K is the Boltzmann constant ($8.617 \times 10^{-5} \text{ eV} \cdot \text{K}^{-1}$).

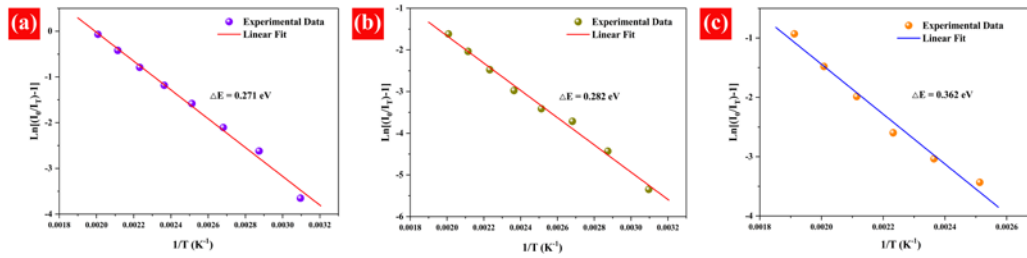


Fig. S6 Plots of $\ln(I_0/I_T - 1)$ versus $1/T$ for the activation energy graph for thermal quenching of the (a) ScLu30Y00, (b) ScLu20Y10 and (c) ScLu15Y15 TCs.

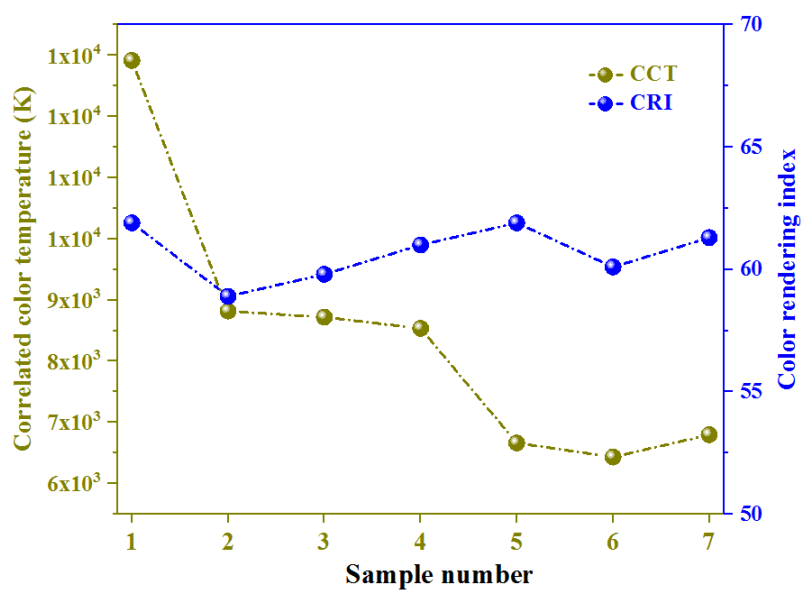


Fig. S7 The detailed CCT and CRI values of Ce:LuYSAG TCs based white LDs.